Charge Transfer Chemistry of Benzo[2,1-*c*:3,4-*c*′]bis(1,2,3-dithiazole) (BT). Preparation and Structural Characterization of [BT][ClO_4] and [BT]$_3$[X]$_2$ (X = ClO_4^- and FSO_3^-)

Tosha M. Barclay,[1a] A. Wallace Cordes,[1a] Richard T. Oakley,*,[1b]
Kathryn E. Preuss,[1b] and Robert W. Reed[1b]

Department of Chemistry and Biochemistry, University of Arkansas, Fayetteville, Arkansas 72701, and Department of Chemistry, University of Waterloo, Waterloo, Ontario N2L 3G1, Canada

Received September 8, 1998. Revised Manuscript Received October 27, 1998

The heterocyclic π-donor benzo[2,1-*c*:3,4-*c*′]bis(1,2,3-dithiazole) (BT) can be prepared in 60% yield by the condensation of 1,4-diaminobenzene-2,3-dithiol with sulfur monochloride. BT is also formed, in low yield, along with its 5-chloro and 5,6-dichloro derivatives, in the reaction of *p*-phenylenediamine with sulfur monochloride. Cyclic voltammetry on BT reveals two reversible oxidation waves at 0.61 and 1.10 V (in CH_3CN, ref SCE). The ESR signal ($g = 2.0175$) of the radical cation BT^+ [in SO_2(l)] exhibits a 1:2:3:2:1 hyperfine structure with $a_N = 0.161$ mT. BT forms radical ion salts by electro-oxidation in the presence of inorganic counterions. In addition to a 1:1 salt [BT][ClO_4], the structure of which consists of a simple ionic arrangement of BT^+ radical cations and ClO_4^- anions, BT also forms 3:2 salts, i.e., [BT]$_3$[X]$_2$, with X = ClO_4^- and FSO_3^-. The crystal structures of these 3:2 salts consist of triple-decker units of radical cation dimers, i.e., $[BT_2]^{2+}$, and neutral BT molecules. These units are packed into ribbonlike arrays interspersed (to either side) by counterions. The ClO_4^- and FSO_3^- salts differ in the way these ribbons are layered on top of one another. Both can be considered as forming slipped π-stacks, but the degree of offset between consecutive layers is considerably larger in the ClO_4^- salt. The room-temperature conductivity of [BT][ClO_4] is ca. 10^{-5} S cm^{-1}, while that of the two 3:2 salts is ca. 10^{-2} S cm^{-1}.

Introduction

Most radical cation conductors are based on variants of the classical organic π-donor tetrathiafulvalene, TTF.[2] A variety of other sulfur-containing heterocycles have been explored as building blocks,[2−4] but purely inorganic donors, such as sulfur nitrogen rings, are absent from this group, in part because the oxidation of binary rings, e.g., S_4N_4, leads to skeletal degradation.[5] Blends of inorganic and organic ring systems can, however, lead to more favorable redox chemistry, and also enhanced intermolecular interactions.[6] In this regard, bifunctional 1,2,3-dithiazoles, or bis(1,2,3-DTA)s, represent a new and potentially valuable class of heterocycle. Recently prepared examples include the 5,5′-fused system **1**[7] and the benzo- and naphtho-bridged derivatives **2** and **3**.[8,9] These antiaromatic ring systems possess closed shell (quinoid) rather than diradical[10] electronic structures,

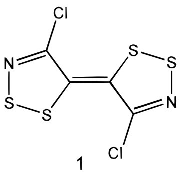
1

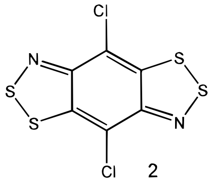
2

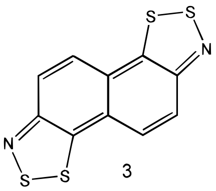
3

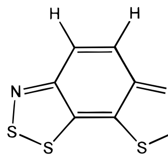
4a, BT

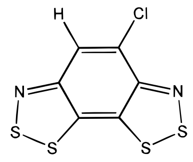
4b, chloro-BT

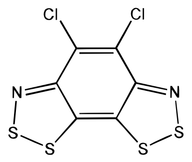
4c, dichloro-BT

---

[1] (a) University of Arkansas. (b) University of Waterloo.

[2] See, for recent reviews (a) Bryce, M. R. *Chem. Soc. Rev.* **1991**, *20*, 355. (b) Gomper, R.; Wagner, H. W. *Angew. Chem., Int. Ed.* **1988**, *27*, 1437. (c) Grossel, M. C.; Weston, S. C. *Contemp. Org. Synth.* **1994**, *1*, 317. (d) Williams, J. M.; Ferraro, J. R.; Thorn, R. J.; Carlson, K. D.; Geiser, U.; Wang, H. U.; Kini, A. M.; Whangbo, M.-H. *Organic Superconductors (Including Fullerenes)*; Prentice Hall: New Jersey, 1992.

[3] (a) Tsubata, Y.; Suzuki, T.; Miyashi T.; Yamashita, Y. *J. Org. Chem.* **1992**, *57*, 6749. (b) Tani, H.; Nii, K.; Maumoto, K.; Azuma, N.; Ono, N. *Chem. Lett.* **1993**, 443.

[4] Yamashita, Y.; Tomura, M. *J. Mater. Chem.* **1998**, *8*, 1933.

[5] Chivers, T.; Hojo, M. *Inorg. Chem.* **1984**, *23*, 4088.

[6] (a) Zambounis, J. S.; Christen, E.; Pfeiffer, J.; Rihs, G. *J. Am. Chem. Soc.* **1994**, *116*, 925. (b) Underhill, A. E.; Hawkins, I.; Edge, S.; Wilkes, S. B.; Varma, K. S.; Kobayyashi, A.; Kobayshi, H. *Synth. Met.* **1991**, *42*, 2093. (c) Tomura, M.; Tanaka, S.; Yamashita, Y.; *Heterocycles* **1993**, *35*, 69.

[7] Barclay, T. M.; Cordes, A. W.; Oakley, R. T.; Preuss, K. E.; Reed, R. W. *J. Chem. Soc., Chem. Commun.* **1998**, 1039.

[8] Barclay, T. M.; Cordes, A. W.; Goddard, J. D.; Mawhinney, R. C.; Oakley, R. T.; Preuss, K. E.; Reed, R. W. *J. Am. Chem. Soc.* **1997**, *119*, 12136.

[9] Barclay, T. M.; Burgess, I. J.; Cordes, A. W.; Oakley, R. T.; Reed, R. W. *J. Chem. Soc., Chem. Commun.* **1998**, 1939.

[10] Genin, H.; Hoffmann, R. *Macromolecules* **1998**, *31*, 444.

10.1021/cm980616b CCC: $18.00

and their chemical and electrochemical oxidation affords stable, highly delocalized radical cations. As such, bis(1,2,3-DTA)s represent promising building blocks for novel radical ion conductors. Indeed, we have recently shown that **3** (NT) forms a mixed valence salt $[NT]_3[BF_4]_2$ with a slipped π-stack structure.[9]

As a development of research on bis(1,2,3-DTA) systems, specifically their use as donors for charge transfer (CT) conductors, we have prepared and structurally characterized benzo[2,1-*c*:3,4-*c*′]bis(1,2,3-dithiazole) (**4a**, BT). Like its structural isomer **2**, BT exhibits a rich redox chemistry, acting as a source of CT salts with a variety of stoichiometries and structures by electro-oxidation. Herein we describe the electrocrystallization and structural characterization of the 1:1 salt $[BT][ClO_4]$ and the two 3:2 salts $[BT]_3[X]_2$ ($X = ClO_4^-$ and FSO_3^-).

Results and Discussion

Synthesis. The Herz reaction, i.e., the cyclocondensation of an aromatic amine with sulfur monochloride, provides an effective synthetic route to 1,2,3-dithiazole derivatives.[11,12] Application of the reaction to aromatic diamines can lead to more complex chemistry. For example, early work on the reaction of *p*-phenylenediamine with sulfur chlorides revealed largely polymeric products.[13] By contrast, the greater reactivity of naphthalene to electrophilic attack (at the peri positions) leads to a relatively clean "double Herz" cyclization. Thus the reaction of 2,6-diaminonaphthalene with sulfur monochloride affords NT (**3**) in good yield.[9] Encouraged by this latter finding, we re-examined the reaction of *p*-phenylenediamine with S_2Cl_2 and found that small amounts of the BT **4a**, along with the chloro-BT and dichloro-BT derivatives **4b** and **4c**, are produced, but in very low (<5%) overall yield. Compound **2** is not produced in this reaction.

To generate BT in chemically more useful quantities, we turned to the use of 1,4-diaminobenzene-2,3-dithiol **5** (as its hydrochloride).[14] We have found that when **5**·2HCl and excess S_2Cl_2 are heated in refluxing chlorobenzene for 3 h, a black precipitate containing what we believe is the chloride salt of the radical cation $[BT]^+$ is produced (eq 1). Reduction of this solid with triphenylantimony in CH_3CN affords the neutral compound BT, which can be recrystallized from toluene as lustrous purple/black needles in an overall yield of nearly 60%. Only trace amounts of the mono- and dichloro-BT compounds **4b** and **4c** are produced in this reaction. Small amounts of the latter compound can be prepared, for characterization purposes, by heating BT in refluxing S_2Cl_2 for 72 h.

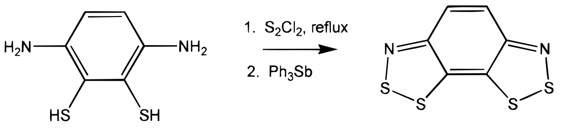

5 4a, BT Eqn 1

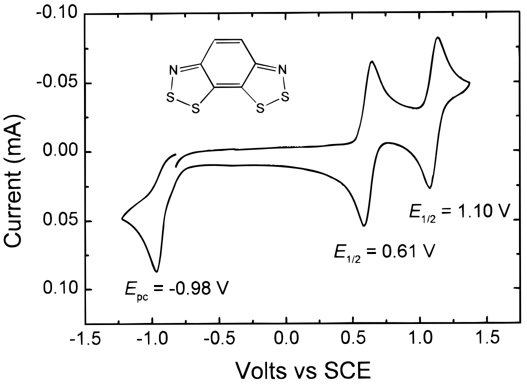

Figure 1. CV scan of BT in CH_3CN, with 0.1 M n-Bu_4NPF_6 supporting electrolyte.

Table 1. Redox Potentials,[a] Visible Absorption Maxima,[b] and ESR Data for Bis(1,2,3-DTA)s

compd	1	2	3	4a	4c
$E_{1/2}^{(0/+)}$	0.80	0.93	0.41	0.61	0.81
$E_{1/2}^{(+/++)}$	1.25	1.5[c]	0.66	1.10	1.37
ΔE	0.45	0.57	0.25	0.49	0.56
$E_{pc}^{(0/-)}$	−1.11	−0.95	−1.06	-0.98	−0.96
λ_{max}	565	525	622	572	600
a_N[d]	0.096	0.201	0.235	0.161	0.143
g value	2.0117	2.0114	2.0106	2.0117	2.0117
$q\pi N$[e]	0.037	0.069	0.063	0.060	0.056
$q\pi S(S)$[e]	0.141	0.106	0.107	0.146	0.146
$q\pi S(N)$[e]	0.175	0.159	0.108	0.149	0.148

[a] Volts vs SCE, in CH_3CN. [b] Nanometers, in CH_2Cl_2 or $C_2H_4Cl_2$. [c] Irreversible; the anodic peak potential E_{pa} is cited. [d] In millitesla, for radical cation. [e] MNDO estimates for radical cation.

Cyclic Voltammetry and ESR Spectra. We have shown previously that bis(1,2,3-DTA)s can be oxidized both chemically and electrochemically to the corresponding radical cations and closed shell dications. Within this context, BT and dichloro-BT behave as expected. Cyclic voltammetry on solutions of either compound in CH_3CN, with $[Bu_4N][PF_6]$ as supporting electrolyte, reveals two reversible oxidation waves and a single irreversible reduction wave (Figure 1). To place the CV data in context, we provide in Table 1 a listing, for all the known bis(1,2,3-DTA)s, of the half-wave potentials [$E_{1/2}$(ox)] of the first and second oxidations as well as the cathodic peak potential (E_{pc}) for the reduction process. Also listed in Table 1 are the electronic absorption maxima (λ_{max} values) of the various compounds. Several conclusions are immediately apparent. For example, the attachment of chlorine substituents to BT has the predictable effect of shifting both $E_{1/2}$(ox) potentials to more anodic values. Likewise, increasing the extent of delocalization by the incorporation of another aromatic ring (as in NT) lowers both the excitation energy and the oxidation potential.

The radical cations of both BT and dichloro-BT have been characterized by ESR spectroscopy. The ESR spectra consist of a pentet with a 1:2:3:2:1 intensity pattern characteristic of hyperfine coupling to two equivalent nitrogens. The a_N constants and *g* values are listed in Table 1, along with calculated (MNDO) spin densities $q\pi$ at sulfur and nitrogen. In general terms, the a_N values for all the bis(1,2,3-DTA)s listed are about one-half the values of those observed in simple monofunctional 1,2,3-DTAs,[12] a difference that can be at-

---

(11) Warburton, W. K. *Chem. Rev.* **1957**, *57*, 1011.

(12) Mayer, R. *Phosphorus Silicon* **1985**, *23*, 277.

(13) Scherer, O. J.; Wolmershäuser, G.; Jotter, *Z. Naturforsch.* **1982**, *37b*, 432.

(14) (a) Green, A. G.; Perkin, A. G. *J. Chem. Soc.* **1903**, *83*, 1201. (b) Lakshmikantham, M. V.; Raasch, M. S.; Cava, M. P. Bott, S. G.; Atwood, J. L. *J. Org. Chem.* **1987**, *52*, 1874.

tributed to the fact that spin delocalization spans two DTA rings rather than one.[15] Similarly the larger g values in bis(1,2,3-DTA) radical cations can be related to the presence of four sulfur atoms rather than two in simple 1,2,3-DTA radicals. Collectively, the trends in a_N and g values correlate well with the calculated spin distributions.

In summary, while the oxidation of BT and other bis-(1,2,3-DTA) systems requires more forcing conditions than, for example, those observed for the oxidation of classical π-donors such as TTF,[16] the ensuing radical cations are extremely stable, highly delocalized, and exhibit substantial spin density on sulfur. These factors, taken together with the small difference ΔE in the first and second oxidation potentials, which can be interpreted in terms of a relatively low Coulombic barrier to charge transfer in the solid state, augur well for the use of these materials as building blocks for radical ion conductors.

Charge-Transfer Salts. To explore the potential of BT in the design of CT conductors, we have carried out a systematic study of its response to electro-oxidation in the presence of simple tetrahedral inorganic counterions, the latter being introduced as 0.1 M solutions of their tetra-*n*-butylammonium salts. We have tested several solvents and a range of current densities, and to date the most effective combination is pure 1,2-dichloroethane with currents of 1−5 μA. While large ($FeCl_4^-$, $GaCl_4^-$) and small (BF_4^-) anions failed to deposit any product under these conditions, the medium-sized anions ClO_4^- and FSO_3^- afforded well-formed crystalline material on the anode within a few days. In the case of FSO_3^- only one morphology, with a 3:2 stoichiometry, i.e., $[BT]_3[FSO_3]_2$, was observed. With ClO_4^-, however, two different crystalline forms, corresponding to 1:1 and 3:2 stoichiometries, i.e., $[BT][ClO_4]$ and $[BT]_3[ClO_4]_2$, were generated. These two morphologies often cocrystallized, rendering their separation a difficult if not impossible task. Fortunately, on several occasions, when using low current densities (1−2 μA), only one of the two forms nucleated and grew. Under these circumstances, isolation of both salts was straightforward. The structural characterization of both the ClO_4^- and the FSO_3^- salts is described below.

To establish a benchmark for the internal structural parameters of the CT salts, we have also determined the crystal structure of neutral BT. It consists of a simple slipped π-stack arrangement of BT molecules running in the x direction (Figure 2), with a cell repeat of 3.9033(8) Å along this direction. Crystal data for BT and the three CT salts are compiled in Table 2. Mean internal structural parameters are summarized in Table 3, and a listing of pertinent intermolecular S···S contacts is provided in Table 4.

$[BT][ClO_4]$. Metallic green blocks of the 1:1 salt $[BT][ClO_4]$ usually grew on the electrode as an impacted mass, but on one occasion a few discrete cubes suitable for single-crystal X-ray analysis were also obtained. The crystals belong to the orthorhombic space group *Pcab* and consist of layers of tilted $[BT]^+$ radical cations interspersed by layers of ClO_4^- anions (Figure 3). This simple ionic packing arrangement (i.e., alternating cations and anions) affords few interannular cation/cation contacts; the shortest intermolecular S···S approach (3.740 Å) is well outside the van der Waals distance (3.6 Å) for two sulfurs.[17] Comparison of the intramolecular distances in neutral BT and its radical cation BT^+ (Table 3) reveal the expected differences; i.e., the S−S, S−N, and S−C bonds are shortened, and the N−C bonds are lengthened by one-electron oxidation.[8] Consistently, the changes are approximately half as large as those previously observed for the two-electron oxidation of **2** (to $[\mathbf{2}][AlCl_4]_2$).[8]

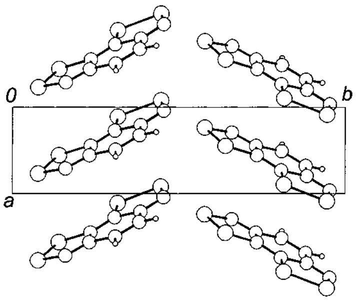

Figure 2. Slipped π-stacks of BT.

$[BT]_3[ClO_4]_2$ and $[BT]_3[FSO_3]_2$. At the molecular level, these two structures share a common building block, a triple-decker slipped π-stack $[BT]_3^{2+}$ unit (Scheme 1) similar to that observed in $[NT]_3[BF_4]_2$.[9] While the 3:2 stoichiometry formally suggests the presence of a $^2/_3+$ charge per heterocyclic ring, comparison of the intramolecular distances in BT (Table 3), $[BT][ClO_4]$ and $[BT]_3[ClO_4]_2$, and $[BT]_3[FSO_3]_2$ leads to the conclusion that two layers in $[BT]_3^{2+}$ are nominally oxidized (the S−S and S−N distances are shorter) to the radical cation level (charge = 1+), while the third layer corresponds to a neutral ring (charge = 0). The radical cations in the first two layers are associated into a dimeric unit, with interannular S···S separations (Table 4) similar to those seen in the $[NT]_3[BF_4]_2$ structure,[9] as well as in other thiazyl radical ion dimers and mixed valence trimers.[18,19]

Although these two 3:2 salts share common features at the molecular level, their crystal structures are quite different. Simple inspection of the crystal morphologies signals this fact; the perchlorate salt forms lustrous purple plates, while the fluorosulfate grows as purple needles. The 3:2 perchlorate salt belongs to the monoclinic space group $P2_1/c$. The asymmetric unit consists of three approximately coplanar BT molecules within the triple decker $[BT]_3^{2+}$ unit (Scheme 1), along with two perchlorate anions, one of which is disordered. The 3:2 fluorosulfate salt belongs to the monoclinic space group $C2/c$. While the *chemical* building block can be considered the same as that found for the 3:2 perchlorate salt, the *crystallographic* building block is actually half this size. The neutral BT molecule is bisected by a

---

[15] Preston, K. F.; Sutcliffe, L. H. *Magn. Reson. Chem.* **1990**, *28*, 189.

[16] (a) Berlinsky, A. J.; Carolan, J. F.; Weiler, L. *Can. J. Chem.* **1974**, *52*, 3373. (b) Kobayashi, T.; Yoshida, Z.; Awaji, H.; Kawase, T.; Yoneda, H. *Bull. Chem. Soc. Jpn.* **1984**, *56*, 2591. (c) Lichtenberger, D. L.; Johnston, R. L.; Hinkelmann, K.; Suzuki, T.; Wudl, F. *J. Am. Chem. Soc.* **1990**, *112*, 3302.

[17] Bondi, A. *J. Phys. Chem.* **1986**, *68*, 441.

[18] Wolmershäuser, G.; Wortmann, G.; and Schnauber, M. *J. Chem. Research (S)* **1988**, 358.

[19] Bryan, C. D.; Cordes, A. W.; Haddon, R. C.; Hicks, R. G.; Oakley, R. T.; Palstra, T. T. M.; Perel, A. S.; Scott, S. R. *Chem. Mater.* **1994**, *6*, 508.

Table 2. Crystal, Data Collection, and Refinement Parameters

compound	BT	[BT][ClO$_4$]	[BT]$_3$[ClO$_4$]$_2$	[BT]$_3$[FSO$_3$]·$^1/_2$(H$_2$O)
formula	$S_4N_2C_6H_2$	$S_4N_2C_6H_2ClO_4$	$S_{12}N_6C_{18}H_6Cl_2O_8$	$S_7N_3C_9H_4O_{3.5}F$
fw	230.33	329.78	889.90	453.59
a, Å	3.9033(8)	11.8155(19)	12.618(2)	16.448(3)
b, Å	14.8321(18)	13.456(3)	18.282(3)	18.322(2)
c, Å	14.068(2)	14.087(2)	13.564(6)	10.534(5)
β, deg	95.835(14)		100.16(2)	106.77(2)
V, Å^3	809.8(2)	2239.7(7)	3079.9(15)	3039.5(16)
d(calcd), g cm^{-3}	1.89	1.96	1.92	1.94
space group	$P2_1/c$	Pcab	$P2_1/n$	$C2/c$
Z	4	8	4	8
temp, K	293	293	293	293
μ, mm^{-1}	1.06	1.06	1.92	1.03
refls in refinement $I > n\sigma(I)$	1102 ($n = 1$)	1427 ($n = 1$)	6350 ($n = 3$)	1769 ($n = 2$)
$R(F)$, $R_w(F)$*	0.045, 0.048	0.056, 0.059	0.066, 0.096	0.055, 0.072

$^*R = [\Sigma||F_o| - |F_c||]/[\Sigma|F_o|]$; $R_w = \{[\Sigma w||F_o| - |F_c||^2]/[\Sigma(w|F_o|^2)]\}^{1/2}$.

Table 3. Summary of Mean Intramolecular Distances (Å)

compound	BT	[BT][ClO$_4$]	[BT]$_3$[ClO$_4$]$_2$		[BT]$_3$[FSO$_3$]$_2$	
formal charge	BT	[BT]$^+$	BT	[BT]$^+$	BT	[BT]$^+$
S−S	2.096(5)	2.060(15)	2.108(17)	2.066(18)	2.108(2)	2.071(15)
S−N	1.646(7)	1.605(5)	1.648(11)	1.62(4)	1.640(5)	1.599(16)
S−C	1.744(8)	1.710(5)	1.731(13)	1.72(3)	1.735(6)	1.719(15)
N−C	1.305(6)	1.311(13)	1.302(12)	1.32(2)	1.308(8)	1.322(12)
(S)C−C(S)	1.356(6)	1.379(8)	1.3849(12)	1.38(3)	1.372(12)	1.390(8)

The numbers in parenthesis represent the larger of the range and the ESD.

Table 4. Intermolecular Contacts (Å) in [BT]$_3$[ClO$_4$]$_2$ and [BT]$_3$[FSO$_3$]$_2$

[BT]$_3$[ClO$_4$]$_2$			
BT$^+$/BT$^+$		BT$^+$/BT	
S5···S9	3.272(4)	S1···S5	3.654(4)
S6···S10	3.399(4)	S2···S6	3.809(4)
S7···S11	3.339(4)	S3···S7	3.784(4)
S8···S12	3.277(4)	S4···S8	3.694(4)
S1···S11′	3.765(4)		
S1···S12′	3.695(4)		
S2···S12′	3.759(4)		
[BT]$_3$[FSO$_3$]$_2$			
BT$^+$/BT$^+$		BT$^+$/BT	
S1···S4′	3.208(3)	S1···S5′	3.790(3)
S2···S3′	3.315(3)	S2···S6′	3.652(3)
S3···S6	3.801(3)		
S4···S5	3.766(3)		

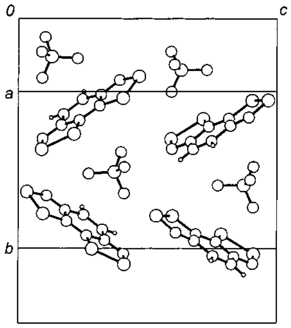

Figure 3. Packing of [BT][ClO$_4$].

2-fold rotation axis, so that the asymmetric unit consists of one-half of the neutral BT molecule and one of the BT$^+$ radical cations. The single FSO$_3^-$ anion is disordered and appears to be associated with what we have refined as a partial water molecule.

The crystallographic differences in the asymmetric units of [BT]$_3$[ClO$_4$]$_2$ and [BT]$_3$[FSO$_3$]$_2$ are coupled to distinct packing patterns for the [BT$_3$]$^{2+}$ molecular building blocks in the two salts. In both structures the [BT$_3$]$^{2+}$ "trimers" align themselves into snakelike arrays or ribbons interspersed with ClO$_4^-$ or FSO$_3^-$ anions on either side (Figure 4). When viewed from the side these ribbons form slipped π-stack arrangements. The key difference between the two structures is the degree of slippage between adjacent levels of these ribbons. In [BT]$_3$[FSO$_3$]$_2$ the slippage (Figure 5) is relatively small, being defined by the 2-fold axis through the neutral BT ring such that translation of successive levels is identical to the slippage between the neutral layer and the radical cation dimer layers within each trimer. By contrast, the lateral translation of the three-layer ribbons in [BT]$_3$[ClO$_4$]$_2$ moves the trimers into an almost completely out-of-register sequence (Figure 5); i.e., trimers with concave curvature are sandwiched above and below by trimers with convex curvature.

Scheme 1

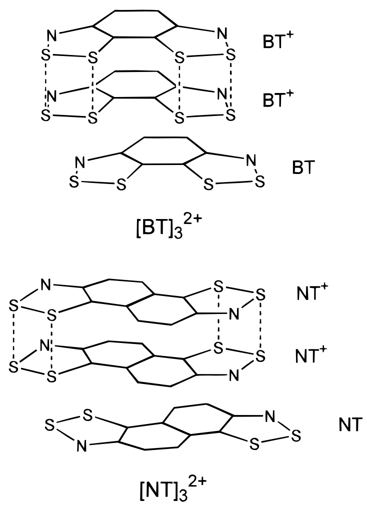

Conductivity. Consistent with the ionic packing pattern in the 1:1 salt [BT][ClO$_4$] and the consequent absence of close intermolecular interactions between cations, electronic communication between neighboring radical cations is small, leading to a narrow bandwidth for the associated energy band. Given that the barrier to charge transfer for a formally half-filled energy band is expected to be high, it is not surprising that the

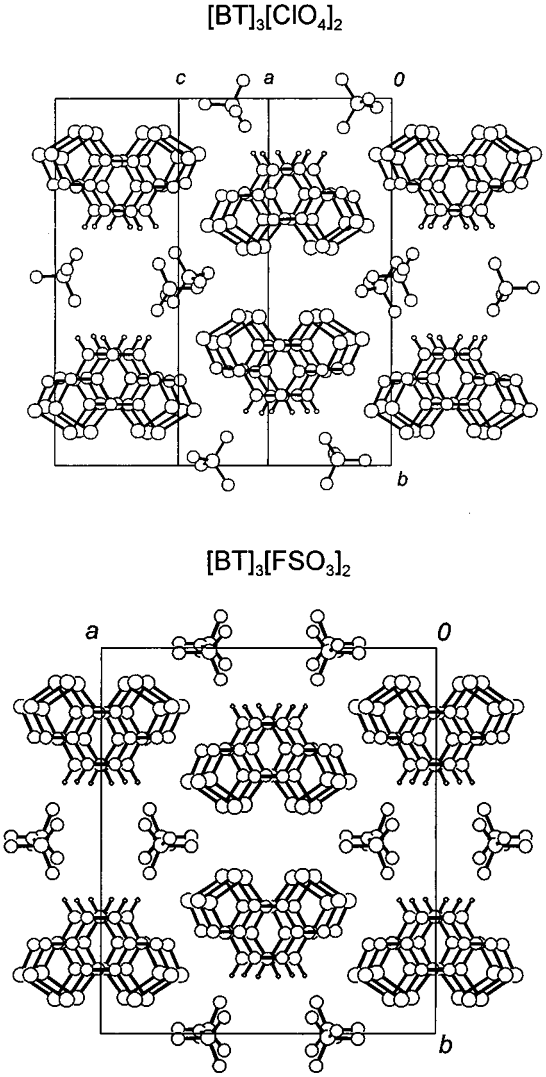
$[BT]_3[ClO_4]_2$

$[BT]_3[FSO_3]_2$

Figure 4. Zigzag arrays of $[BT]_3^{2+}$ in $[BT]_3[ClO_4]_2$ (above) and $[BT]_3[FSO_3]_2$ (below). For purposes of clarity, only one of the models used for the disordered ClO_4^- and FSO_3^- anions is shown.

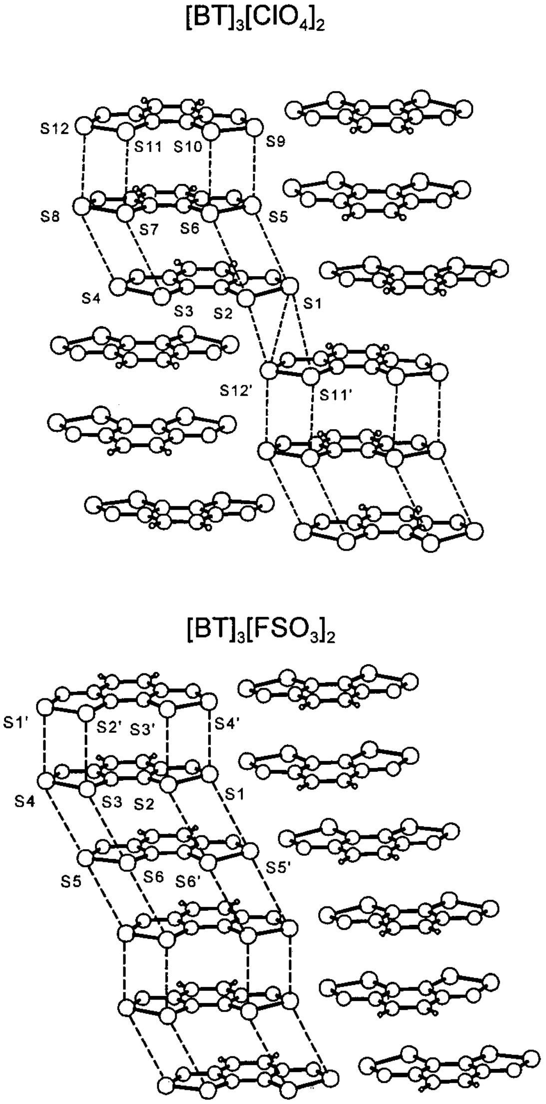
$[BT]_3[ClO_4]_2$

$[BT]_3[FSO_3]_2$

Figure 5. Stacking of $[BT]_3^{2+}$ in $[BT]_3[ClO_4]_2$ (above) and $[BT]_3[FSO_3]_2$ (below). The anions have been omitted for purposes of clarity. S···S contacts are defined in Table 4.

pressed pellet conductivity of $[BT][ClO_4]$ is ca. 10^{-5} S cm^{-1}; the material behaves as a Mott insulator. In the 3:2 salts the two components of the triple decker $[BT_3]^{2+}$, the radical cation dimer $[BT_2]^{2+}$, and the neutral molecule BT are individually closed shell, so that the electronic structure of the whole is expected to mimic that of a small band gap semiconductor. Consistently both $[BT]_3[ClO_4]_2$ and $[BT]_3[FSO_3]_2$ exhibit pressed pellet conductivities of ca. 10^{-2} S cm^{-1} at room temperature, values similar to that found for $[NT]_3[BF_4]_2$.[9]

Summary and Conclusions

The bis(1,2,3-DTA) framework provides a flexible template for the design of CT molecular conductors. While the oxidation potentials of bis(1,2,3-DTA) derivatives are generally higher than those encountered in traditional organic π-donors, the resulting radical cations are extremely stable, are highly delocalized, and have exposed peripheries capable of strong intermolecular interactions. Moreover, the energetics of disproportionation of the radical cations to the corresponding dications and neutrals is comparable to that seen in TTF-type materials, suggesting that the barrier to charge transfer should be similar. The present work establishes that bis(1,2,3-DTA)s are capable of forming a variety of stable radical ion salts with inorganic counterions. In the 1:1 salt of BT, conductivity is limited by the relative isolation of the radical cations. The triple-decker π-stacked 3:2 salts of BT and NT are more conductive, but the cofacial dimerization of two radical cations opens a gap at the Fermi level, and the materials are semiconductors. It remains to be seen if this form of dimerization can be suppressed, either by the attachment of peripheral substituents that inhibit perfectly cofacial approach or by the design of larger, more delocalized bridging groups, which allow for the development of more two- and three-dimensional interactions. The effects of replacement of sulfur by selenium[8] can also be explored.

Experimental Section

General Procedures and Starting Materials. Sulfur monochloride, *p*-phenylenediamine, and triphenylantimony were obtained commercially (Aldrich) and used as received. The electrolytes $[n\text{-}Bu_4N][X]$, with $X^- = BF_4^-$, PF_6^-, and ClO_4^-, were also obtained commercially (Fluka) and used as received, while for $X^- = GaCl_4^-$ and FSO_3^- the materials were prepared and purified according to literature procedures.[20] The diaminobenzenedithiol **5** (as its dihydrochloride) was also prepared according to standard literature methods.[14] The solvents chlorobenzene (Fisher), dichloroethane (Fisher), and acetonitrile (Fisher HPLC grade) were commercial products and dried by distillation from P_2O_5. All reactions were carried out under an atmosphere of nitrogen. Fractional sublimations of **4a**, **4b**, and **4c** were performed in an ATS series 3210 three-zone tube furnace, mounted horizontally, and linked to a series 1400 temperature control system. Melting points are uncorrected. Elemental analyses were performed by MHW Laboratories, Phoenix, AZ. Infrared spectra were recorded (at 2 cm^{-1} resolution on Nujol mulls) on a Nicolet 20SX/C infrared spectrometer. Low-resolution mass spectra (70 eV, EI, DEI and CI, DCI) were run on a Finnigan 4500 quadrupole mass spectrometer at the McMaster Regional Centre for Mass Spectrometry. X-band ESR spectra of the radical cations of BT **4a** and dichloro-BT **4c** were recorded, using a Varian E-109 spectrometer with DPPH as a field marker, on samples of their radical ion salts, prepared electrochemically and dissolved in SO_2(l). UV−visible spectra were recorded on a Perkin-Elmer Lambda 6 spectrophotometer.

Reaction of *p*-Phenylenediamine with S_2Cl_2. This reaction was performed many times with variations in temperature, solvent, and auxiliary base. The following description represents one of the more successful combinations. A mixture of *p*-phenylenediamine (2.06 g, 19.0 mmol) and excess S_2Cl_2 (12 mL) in 100 mL of CH_2Cl_2 was stirred overnight at room temperature. Pyridine (20 mL) was then added and the mixture again left to stir overnight. A dark brown precipitate was filtered off, washed with CH_2Cl_2 (2 × 100 mL) and CH_3CN (2 × 100 mL), and dried in vacuo. To the solid was then added a solution (200 mL) of 10% ethanol in CH_2Cl_2, and the slurry stirred vigorously for 12 h. The mixture was filtered and the residual solid twice more re-extracted as before. The combined extracts were evaporated to leave a dark semisolid that was dissolved in 100 mL of CH_2Cl_2 and filtered through a small (50 mL) plug of silica. Analysis of the purple filtrate by TLC (SiO_2, CH_2Cl_2) showed the presence of purple ($R_f = 0.65$) and two almost coincident blue materials ($R_f = 0.69$ and 0.70). The purple component (75 mg) was BT, **4a** (see below for full characterization), which could be separated by column chromatography (SiO_2, 3:1 hexane:$CHCl_3$), but the two blue components (combined weight 40 mg) were inseparable by column chromatography. Fractions enriched in one or the other were evaporated and analyzed by mass spectrometry, which indicated the presence of monochloro-BT, **4b** ($R_f = 0.70$), and dichloro-BT, **4c** ($R_f = 0.69$). Because of its lower solubility and lower vapor pressure, small quantities of pure dichloro-BT (**4c**) could be obtained by fractional sublimation at 120−90 °C/10^{-2} Torr followed by recrystallization from hot toluene as bronze blocks. Mp: 248−251 °C. UV−vis ($C_2H_4Cl_2$), λ_{max} (log ϵ): 600 (4.1), 346 (4.4) nm. Anal. Calcd for $C_6Cl_2N_2S_4$: C, 24.08; N, 9.36. Found: C, 24.41; N, 9.28. MS: *m/z* (%) 298 (100). IR (Nujol): ν = 1500 (w), 1410 (w), 1151 (s), 1029 (m), 783 (vs), 738 (m), 663 (vs), 635 (m), 583 (w), 509 (s) cm^{-1}.

Reaction of 5·2HCl with Sulfur Monochloride. A slurry of 1,4-diaminobenzene-2,3-dithiol dihydrochloride (**5**·2HCl) (1.00 g, 4.05 mmol) and excess S_2Cl_2 (5 mL) was heated in refluxing chlorobenzene for 3 h. The mixture was cooled to room temperature and the black precipitate of crude [BT][Cl] filtered off, washed with 2 × 10 mL chlorobenzene, and dried in vacuo. This material was then reduced by heating it at reflux in 40 mL of CH_3CN containing excess triphenylantimony (1.43 g, 4.05 mmol). Filtration of this mixture afforded crude product, BT, which was extracted into toluene (4 × 50 mL). Evaporation of the extracts and recrystallization from hot toluene afforded pure BT as lustrous purple-black needles (0.55 g, 2.4 mmol, 59%). Mp: 187−189 °C. UV−vis (CH_2Cl_2), λ_{max} (log ϵ): 572 (4.2), 329 (4.0) nm. Material for electrocrystallization work was further purified by fractional sublimation at 100−60 °C/10^{-2} Torr. Anal. Calcd for $C_6H_2N_2S_4$: C, 31.29; H, 0.88; N, 12.16. Found: C, 31.53, H, <0.05; N, 12.08. MS: *m/z* (%) 230 (70, M^+), 133 (24), 88 (40), 76 (100). IR (Nujol): ν = 1391 (w), 1317 (w), 1298 (m), 1122 (w), 1071 (m), 806 (s), 790 (vs), 767 (m), 707 (vs), 592 (m) 525 (m), 471 (m) cm^{-1}.

Preparation of 4c from 4a. A slurry of BT (**4a**, 0.35 g, 1.52 mmol) was heated at reflux in 10 mL of neat S_2Cl_2 for 72 h. The resulting black solid was filtered off, washed with 3 × 20 mL of $C_2H_4Cl_2$, and dried in vacuo. This solid was then reduced by heating it at reflux in 40 mL of CH_3CN containing excess triphenylantimony (0.54 g, 1.52 mmol). Filtration of this mixture afforded a black solid (0.2 g) which, by TLC analysis, was ca. 20% **4b** and 80% **4c**. Pure dichloro-BT **4c** (50 mg) was separated from this mixture by fractional sublimation at 110−80 °C/10^{-2} Torr, followed by crystallization from toluene.

Cyclic Voltammetry. Cyclic voltammetry was performed on a PAR 273A electrochemical system (EG&G Instruments) with scan rates of 50−100 mV s^{-1} on solutions of BT and dichloro-BT containing 0.1 M tetra-*n*-butylammonium hexafluorophosphate in CH_3CN (dried by distillation from P_2O_5). Potentials were scanned from −2.5 to 1.5 V with respect to the quasireference electrode in a single compartment cell fitted with Pt electrodes and referenced to the ferrocenium/ferrocene couple at 0.38 V vs SCE.[21]

Electrocrystallizations. The electrocrystallization work employed standard H-cell techniques,[22] with samples of BT (10 mg) dissolved under nitrogen in 20 mL of solvent containing 0.02−0.05 M [n-Bu_4N][X] ($X^- = BF_4^-$, $GaCl_4^-$, FSO_3^-, and ClO_4^-). The use of mixed solvent systems, e.g., 1:1 $C_2H_4Cl_2$ with CS_2 or PhCl, was explored, and while these less polar mixtures favored the growth of the 3:2 perchlorate salt over the 1:1 version, the largest crystals, certainly those used for X-ray work, were grown from pure $C_2H_4Cl_2$. Currents ranged from 1 to 5 μA, with growth periods of 10−14 days. Crystals of all the CT salts prepared were stable in air.

X-ray Measurements. X-ray data were collected on ENRAF-Nonius CAD-4 with monochromated Mo Kα radiation. Crystals were mounted on glass fibers with silicone or epoxy. Data were collected using a $\theta/2\theta$ technique. The structures were solved using direct methods and refined by full-matrix least squares which minimized $\sum w(\Delta F)^2$.

Electronic Structure Calculations. MNDO calculations were carried out on a Pentium PC using the MOPAC93 suite of programs[23] compiled to run under DOS. All geometries were optimized within the constraints of C_{2h} (**1**, **2**, **3**) and C_{2v} (**4a** and **4c**) symmetry. Spin densities $q\pi$ refer to the square of the pπ-orbital coefficients in the SOMO.

Acknowledgment. We thank the NSERC (Canada) and the NSF/EPSCoR program for financial support. We also acknowledge the NSERC for a postgraduate scholarship to K.E.P. and the Department of Education for a doctoral fellowship to T.M.B.

Supporting Information Available: Tables of crystal data, structure solution and refinement, bond lengths and angles, and anisotropic thermal parameters for the structures reported (22 pages); observed and calculated structure factors (68 pages). Ordering information is given on any current masthead page.

CM980616B

---

[20] (a) Taylor, M. J.; Tuck, D. G. *Inorg. Synth.* **1983**, *22*, 135. (b) Cox, D. D.; Ball, G. A.; Alonso, A. S.; Williams, J. M. *Inorg. Synth.* **1989**, *26*, 393.

[21] Boeré, R. T.; Moock, K. H.; Parvez, M. *Z. Anorg. Allg. Chem.* **1994**, *620*, 1589.

[22] (a) Ferraro, J. R.; Williams, J. M. In *Introduction to Synthetic Electrical Conductors*; Academic Press: New York, 1987; p 25. (b) Stephens, D. A.; Rehan, A. E.; Compton, S. J.; Barkhau, R. A.; Williams, J. M. *Inorg. Synth.* **1986**, *24*, 135.

[23] MOPAC93, Quantum Chemistry Program Exchange.